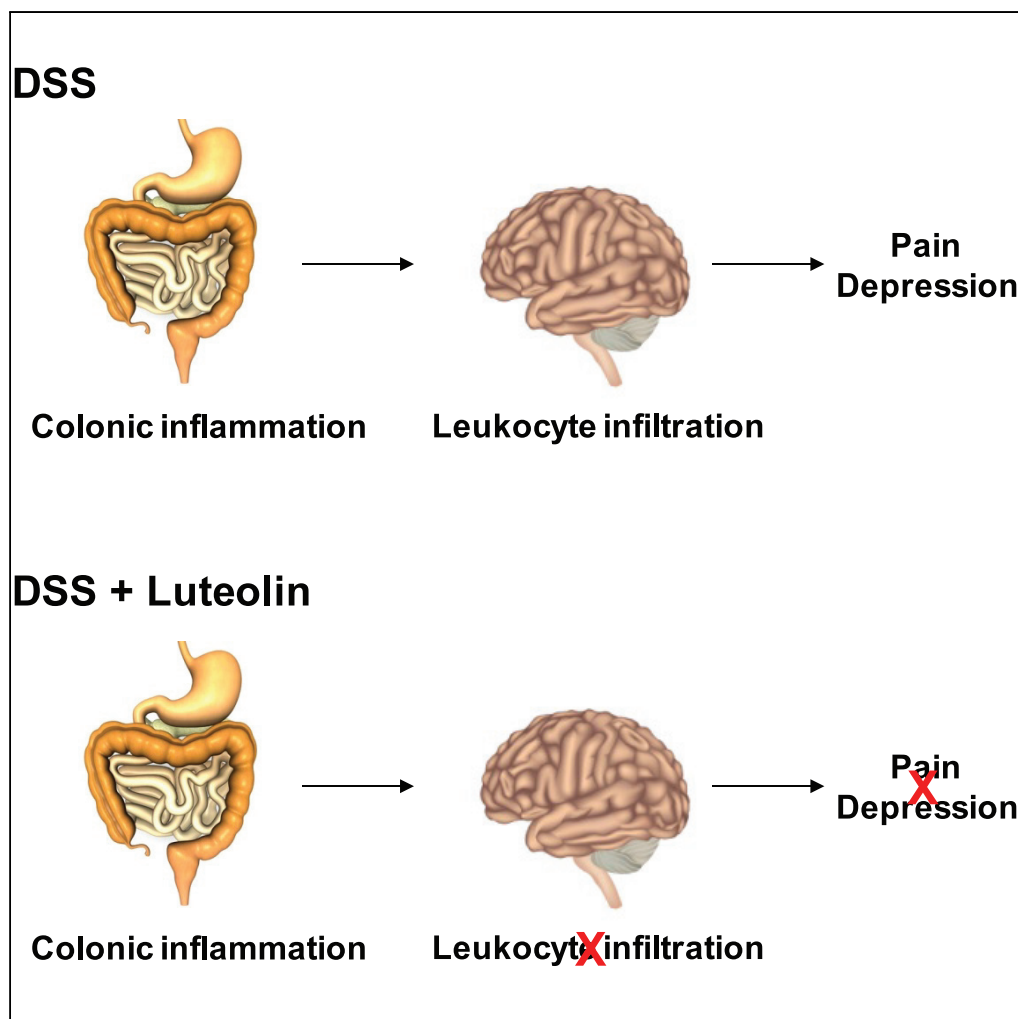


Article

Neuroimmune Responses Mediate Depression-Related Behaviors following Acute Colitis



Vinicius M. Gadotti, Graciela Andonegui, Zizhen Zhang, ..., Wallace K. MacNaughton, Paul Kubes, Gerald W. Zamponi

vgadotti@ucalgary.ca (V.M.G.)
zamponi@ucalgary.ca (G.W.Z.)

HIGHLIGHTS

Acute colitis triggers long-term events related to depression

Leukocytes infiltrate into brain vasculature

Luteolin abolishes leukocyte infiltration and visceral hypersensitivity

Luteolin abolishes depression-related behaviors

Gadotti et al., iScience 16, 12–21
June 28, 2019 © 2019 The Author(s).
<https://doi.org/10.1016/j.isci.2019.05.012>

Article

Neuroimmune Responses Mediate Depression-Related Behaviors following Acute Colitis

Vinicius M. Gadotti,^{1,2,*} Graciela Andonegui,³ Zizhen Zhang,^{1,2} Said M'Dahoma,^{1,2} Cristiane H. Baggio,³ Lina Chen,^{1,2} Lilian Basso,^{1,2,3} Christophe Altier,^{1,2,3} Wallace K. MacNaughton,³ Paul Kubes,³ and Gerald W. Zamponi^{1,2,4,*}

SUMMARY

Many patients with visceral inflammation develop pain and psychiatric comorbidities such as major depressive disorder, worsening the quality of life and increasing the risk of suicide. Here we show that neuroimmune activation in mice with dextran sodium sulfate-induced colitis is accompanied by the development of pain and depressive behaviors. Importantly, treatment with the flavonoid luteolin prevented both neuroimmune responses and behavioral abnormalities, suggesting a new potential therapeutic approach for patients with inflammatory bowel diseases.

INTRODUCTION

Gastrointestinal inflammation during inflammatory bowel diseases (IBDs) involves the activation of immune responses that lead to the release of inflammatory mediators, such as cytokines and chemokines (Strober and Fuss, 2011). This, in turn, gives rise to recurrent visceral pain and causes the development of psychiatric comorbidities such as mood disorders (Walker et al., 2013). Indeed, up to 80% of patients with IBD suffer from anxiety symptoms and 60% develop major depressive disorder (MDD) that often outlasts the resolution of pain symptoms and leads to an increased risk of suicide (Chen et al., 2015). These comorbidities have a major detrimental impact on the quality of life of these patients, but the underlying cellular and molecular mechanisms have not been determined. Although symptoms of depression can potentially be treated with antidepressants (Murrough et al., 2017), a clear unmet need is the ability to prevent the development of psychiatric disorders in patients suffering from inflammatory conditions affecting the gastrointestinal tract.

Functional magnetic resonance imaging studies in patients with IBD have revealed changes in the activity of a number of different brain regions, including the prefrontal cortex (PFC) and hippocampus (Ma et al., 2015; Bao et al., 2016). Among these, the hippocampus is a key brain region within the limbic system that has been linked to depression in both humans and rodents (Dantzer et al., 2008), and during depressive states, there is a dysregulation of several neurotransmitter systems such as the serotonergic, noradrenergic, and GABAergic systems. mRNA levels of specific inflammatory markers, such as for COX-2, are upregulated in the hippocampus of mice with visceral inflammation (Do and Woo, 2018), and prolonged pharmacologically induced visceral inflammation gives rise to reduced hippocampal neurogenesis (Zonis et al., 2015). In addition, there is an inflammatory component to depression, as evident from alterations of interleukin 1 beta (IL-1 β) and tumor necrosis factor alpha (TNF- α) levels in the limbic system of patients with depression (Hodes et al., 2015). Furthermore, anti-inflammatory drugs can be effective in treating comorbid depression-like symptoms in patients with inflammatory disorders (for review see, Hodes et al., 2015). In rodents, both IL-1 β (Ikegaya et al., 2003) and TNF- α (Batti and O'Connor, 2010) have been shown to alter synaptic plasticity in CA1 pyramidal cells.

We therefore reasoned that during visceral inflammation, central nervous system action of inflammatory cytokines released by peripherally activated leukocytes may give rise to alterations in brain function, which in turn lead to neuropsychiatric consequences such as depression. To examine this issue, we employed the dextran sodium sulfate (DSS) model of visceral inflammation. This model is pertinent as it primarily involves the innate immune response and is characterized by inflammatory cell infiltration (along with weight loss, bloody diarrhea, epithelial cell damage) and increased production of inflammatory mediators such as TNF α , IL-6, IL-1, and interferons (primarily the innate immune response) (Lopes et al., 2018). We find that mice treated with DSS develop visceral inflammation and depression-like behaviors. Mice undergoing

¹Department of Physiology and Pharmacology, Hotchkiss Brain Institute, Cumming School of Medicine, University of Calgary, Calgary, AB, Canada

²Department of Physiology and Pharmacology, Children's Hospital Research Institute, Cumming School of Medicine, University of Calgary, Calgary, AB, Canada

³Department of Physiology and Pharmacology, Snyder Institute for Chronic Disease, Cumming School of Medicine, University of Calgary, Calgary, AB, Canada

⁴Lead Contact

*Correspondence: vgadotti@ucalgary.ca (V.M.G.), zamponi@ucalgary.ca (G.W.Z.)

<https://doi.org/10.1016/j.isci.2019.05.012>



DSS treatment display immune cell infiltration into the brain microvasculature that is accompanied by an elevation of IL-1 β levels. The natural flavonoid luteolin prevents both the neuroimmunological events and the development of depression.

RESULTS

We used a 6-day treatment of DSS in drinking water as an experimental model of inflammatory colitis in mice. This model was chosen because DSS disrupts the epithelial barrier, which causes mucosal infection from commensal bacteria and thus colonic inflammation (Lopes et al., 2018). Compared with vehicle-treated animals, DSS mice exhibited reduced body weight over the study time course of 1 month (Figure S1A) and significant neutrophil migration to the colon up to 2 weeks following DSS discontinuation, as revealed by a myeloperoxidase assay (Figure S1B). Mice treated with DSS developed visceral hypersensitivity (see below) that was evident for a week following DSS treatment. Different cohorts of mice were treated with DSS and then tested for depression-related behaviors. We focused predominantly on two time periods. One set of experiments was designed to examine the early responses to DSS during the inflammatory phase, including measurements of gut permeability; measurements of leukocyte infiltration, which is expected to occur during the inflammatory phase; visceral hypersensitivity, which is known to resolve before the 4-week time point (Costa et al., 2012); and weight gain as a function of time after DSS treatment (up to four weeks, see above). To examine the long-term effects of DSS on behavior and associated neurochemical changes, experiments on comorbidities with depression were typically conducted 4 weeks after the discontinuation of DSS, including all critical behavioral measurements for depression, the electrophysiology, and PCR measurements. Figure S2 depicts a summary of the time lines used in this study.

Onset of Depression-Related Behaviors in Male and Female Mice

In the novelty suppressed feeding test, a conflict paradigm test based on hyponeophagia, which is among the most commonly used test for screening of novel antidepressants, both male and female mice subjected to acute visceral inflammation displayed increased latency to interact with food (Figure 1A). Two-way ANOVA revealed a significant difference following DSS treatment ($F(1,99) = 3.3$; $p = 0.0058$) without sex differences in our observations. The effect of DSS treatment on the loss of self-care and motivational behavior was inferred by the time spent grooming in the splash test. The results show decreased time spent grooming for DSS-treated mice (Figure 1B). Two-way ANOVA revealed significant differences in response to DSS treatment ($F(0,64) = 3.4$; $p < 0.0001$) and for the sex versus DSS treatment interaction ($F(1,88) = 11.10$; $p < 0.0179$). Next, we verified whether DSS treatment affects the immobility time in models of depression-related behavior induced by despair. Both the forced swimming test (FST) and the tail suspension test (TST) are used to evaluate depression-related behaviors in rodents, with immobility time being decreased by classical antidepressants (Steru et al., 1985). DSS-treated mice exhibited a significantly elevated immobility time in both FST (Figure 1C) and TST (Figure 1D) compared with control groups for both sexes. Two-way ANOVA showed statistical differences in response to DSS treatment ($F(1,06) = 3.4$; $p < 0.0001$) and for the sex versus DSS treatment interaction ($F(2,16) = 10.9$; $p < 0.0001$) for FST. For the TST, a difference in response to DSS treatment was revealed ($F(1,82) = 3.3$; $p = 0.0022$). All groups of mice displayed normal ambulatory behavior in the open field when assessed at the same time points (between 3 and 4 weeks) as for the FST and TST with no differences found in the number of crossings for either DSS (H₂O versus DSS) or sex (data not shown), thus suggesting that the depression-related behavior of DSS-treated mice was not due to motor deficits. The tricyclic antidepressant imipramine reversed the DSS effects in the TST (Figure 1E). Two-way ANOVA showed statistical differences following DSS treatment ($F(3,82) = 8.8$; $p = 0.0125$) and for the DSS versus imipramine treatment interaction ($F(6,72) = 8.8$; $p < 0.0001$). Collectively, our data show that mice with experimental colitis show a comorbid depression-like phenotype that is consistent with what is observed in patients with IBD. Because similar findings were obtained in both male and female mice, we focused on male mice for all ensuing experiments to reduce the numbers of mice required.

Changes in Electrophysiological Properties and Gene Expression in the Hippocampus

We then performed an electrophysiological analysis of hippocampal neuron function using hippocampal slices. We measured the magnitude of evoked inhibitory post-synaptic currents (IPSCs) in CA1 pyramidal cells in response to electrical stimulation of Schaffer collaterals at a range of stimulus intensities. We found that IPSCs recorded from pyramidal neurons of DSS-treated animals 4 weeks after DSS discontinuation

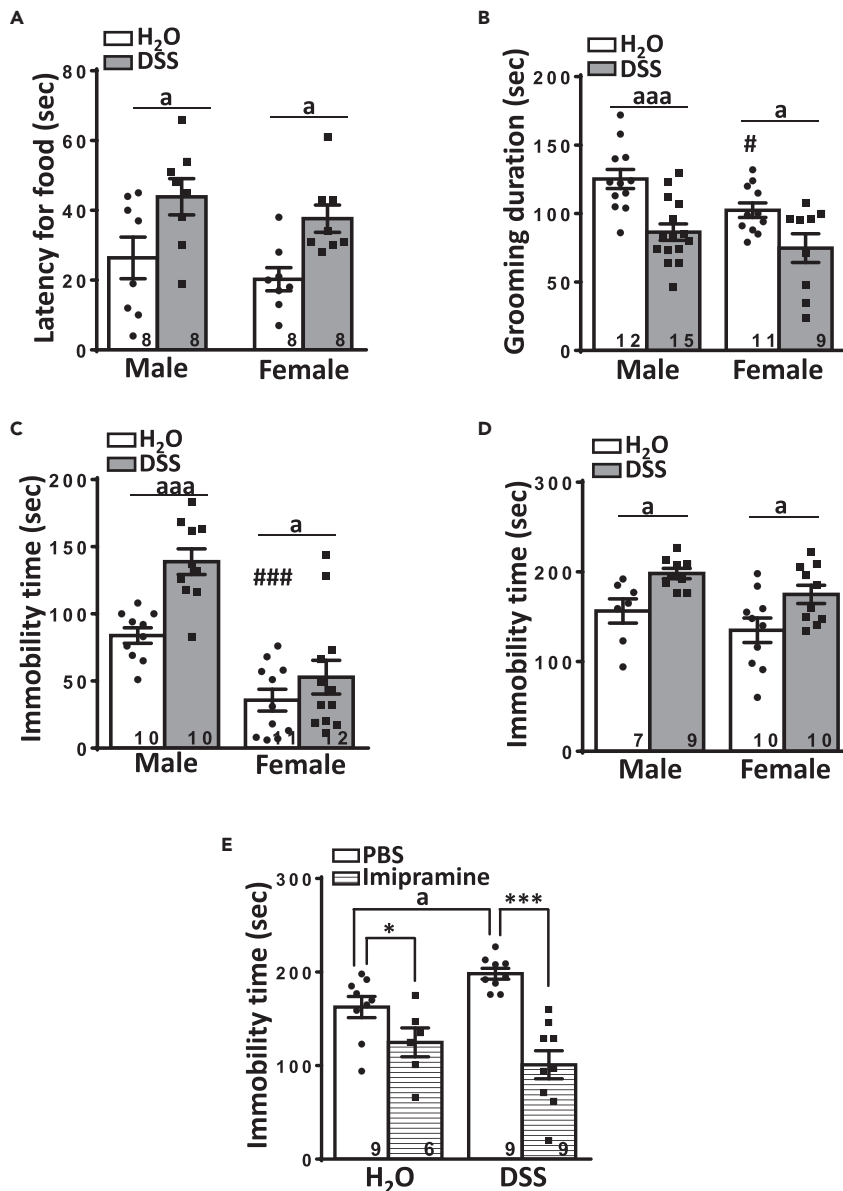


Figure 1. Development of Depression-Related Behaviors Following Acute Colitis

(A–D) (A) Novelty suppressed feeding test, (B) splash test, (C) forced swimming test, and (D) tail suspension test.

(E) Effect of imipramine (10 mg/kg, intraperitoneally) in male mice treated with DSS in the tail suspension test. Each bar represents the mean \pm SEM, numbers depicted in the bars represent numbers of mice tested. The experimenter was blinded to the groups during splash test and forced swimming test.

Two-way ANOVA reveals behavioral abnormalities of mice treated with DSS; ^a $p < 0.05$, ^{aaa} $p < 0.001$ DSS- versus H₂O-treated groups; [#] $p < 0.05$, ^{###} $p < 0.001$ male versus female mice interaction; ^{*} $p < 0.05$, ^{***} $p < 0.001$ imipramine- versus vehicle-treated mice.

were significantly increased in magnitude compared with vehicle-treated animals (Figure 2). Two-way repeated measures (RM) ANOVA revealed statistical differences after DSS treatment ($F(5,85) = 5.5$; $p = 0.0206$). These data suggest the possibility that CA1 pyramidal cells may be under augmented inhibitory control and are consistent with the known involvement of the hippocampus in depressive states (Boddum et al., 2016).

We then performed quantitative PCR analysis of hippocampal tissue at the same time point (4 weeks), and this experiment revealed an elevation of IL-1 β mRNA (Figure 3A), but curiously no changes in TNF- α mRNA

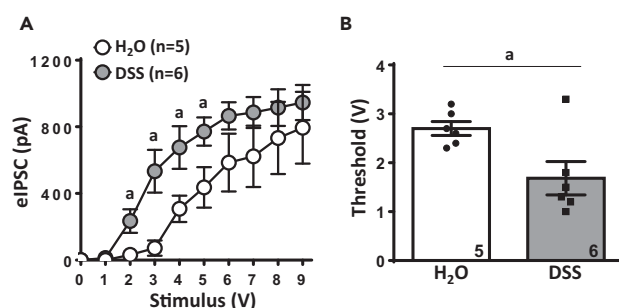


Figure 2. Electrophysiological Properties of the Hippocampus Following Colitis

(A) Whole-cell patch clamp 4 weeks after end of DSS reveals that evoked Inhibitory Post Synaptic Current (eIPSCs) in pyramidal cells of the CA1 area were enhanced and (B) the eIPSC threshold is lower in mice following acute colitis. Each circle (left) and bar (right) represents the mean \pm SEM. Two-way RM ANOVA shows that the feedforward inhibitory synaptic transmission is enhanced in Schaffer collateral input of hippocampal CA1 of mice following inflammatory colitis. * $p < 0.05$.

levels (Figure 3B). Nonetheless, the persistent upregulation of IL-1 β levels suggest a sustained inflammatory process in the brains of DSS-treated mice and is consistent with previous reports implicating this cytokine in depression in rodents (Alcocer-Gómez et al., 2017) and humans (Kolaczowska and Kubes, 2013). Possible microglia activation was characterized by flow cytometry. Activated microglia are identified as CD11b⁺CD45^{intermediate}-expressing cells as described previously (Andonegui et al., 2018). Analysis of total brain samples showed no activation of microglial cells 1 week following DSS discontinuation (Figure 3C), thus indicating that the elevated IL-1 β mRNA levels are not dependent on microglial activation.

Altogether these data indicate that there are persistent changes in gene expression and functional properties in the hippocampus.

Live Imaging of Infiltrating Leukocytes into the Brain Microcirculation

Enhanced IL-1 β in the brain of DSS mice and the lack of microglial activation inspired us to verify leukocyte recruitment in the brain microcirculation by using CX3CR1^{GFP/WT} CCR2^{RFP/WT} mice to track inflammatory and patrolling monocytes. These mice were additionally injected with antibody to label neutrophils. At 7 days after DSS discontinuation, there were no leukocytes in the brain microvessels of the PFC of control mice. However, DSS mice displayed a significant increase in neutrophils and both classical (CCR2^{hi}CX3CR1^{low}) and patrolling (CCR2^{low}CX3CR1^{hi}) monocytes (Figure 4A, 4B, 4D, and 4E and Videos S1 and S2). Importantly, as there appeared to be no activation of microglia, this experiment further confirmed our flow cytometry analysis. Neutrophils mainly mediate tissue damage through activation by cytokines and release of oxidants, proteases, and other factors (de Oliveira et al., 2016). They are thought to re-enter the circulation through reverse neutrophil migration, thus potentially disseminating inflammation and causing damage far away from the original site of injury (Kolaczowska and Kubes, 2013). The observation that an elevated number of neutrophils and monocytes were found in the brain microcirculation after inflammation of the gut supports the concept of long-lasting neuroimmune regulation of brain properties that may be correlated with the behavioral abnormalities found in DSS mice. Moreover, the inflamed blood-brain barrier (BBB) endothelium is known to exhibit increased cytokine expression such as IL-1 β and TNF- α , which contribute to modulate the permeability of the BBB and the phenotype of infiltrating leukocytes (Shechter et al., 2013).

Luteolin Prevents Leukocyte Infiltration, Visceral Pain, and Depression-Related Behavior

Flavonoids are commonly present in a wide range of plants used in traditional medicine to treat a number of disorders and often exhibit anti-inflammatory properties (Spagnuolo et al., 2018). The bioflavonoid luteolin is found in many plants such as peppermint, artichokes, peppers, and carrots and is known to exhibit anti-oxidant, anti-microbial, anti-allergic, neuroprotective, anti-diabetic, and cardioprotective properties (López-Lázaro, 2009). Most importantly, its potent anti-inflammatory actions have been reported both *in vitro* and *in vivo* and appear to be related to its inhibitory action of transcription factors such as nuclear factor (NF)- κ B, inducible nitric oxide synthase (iNOS), and inhibition of the protein kinase B and mitogen-activated protein kinase pathways (Aziz et al., 2018). We thus evaluated its effect on DSS-induced

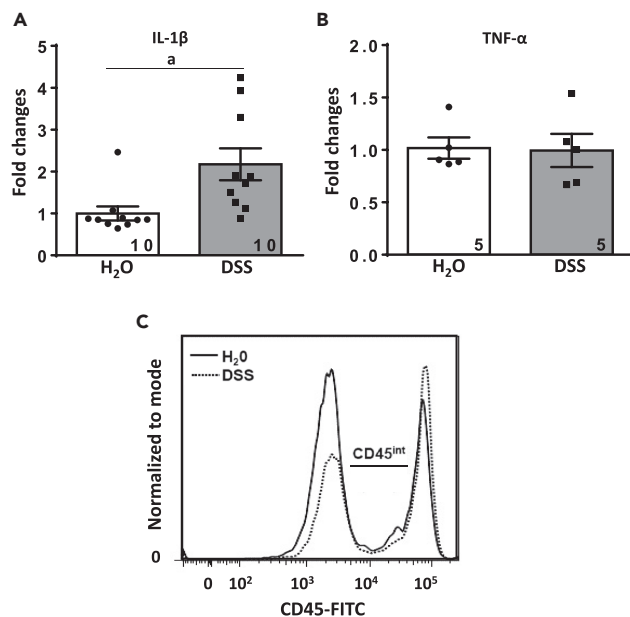


Figure 3. Expression of Genes Related to Inflammation and Depression

(A and B) qPCR quantification of (A) IL-1 β and (B) TNF- α mRNA expression from total hippocampus of mice isolated 4 weeks after discontinuation of DSS or vehicle treatment. Bars represent the mean \pm SEM and are representative of two independent experiments. A t test reveals increased IL-1 β mRNA expression in mice treated with DSS. * $p < 0.05$. (C) Microglia CD11b⁺CD45 intermediate expression by flow cytometry 1 week after DSS discontinuation. Total brain cells from H₂O- and DSS-treated mice were isolated and labeled. The CD11b⁺ cells were gated and analyzed for CD45 intermediate expression. The representative histogram shows that there is no increase in CD45 intermediate (CD45^{int}) expression in the brains of DSS-treated mice (4.685 ± 0.459) when compared with H₂O-treated animals (5.395 ± 0.060). Numerical values represent the mean \pm SEM and are representative of three mice per group.

physiological changes in mice. Treatment of mice with luteolin (15 mg/kg, intraperitoneally, once daily for 15 days starting 2 days before the beginning of DSS treatment) abolished invasion of rolling (Figures 4C and 4D) and adhesion monocyte (Figures 4C and 4E) as well as rolling neutrophils, thus showing a near-complete prevention of leukocyte infiltration into brain microvasculature 1 week after DSS discontinuation (Video S3). Two-way ANOVA showed a significant difference due to DSS treatment ($F(378,0) = 5.5$; $p = 0.0017$) and for the DSS versus luteolin treatment interaction ($F(6,96) = 5.4$; $p = 0.0341$) for rolling monocytes, and for adhesion monocytes (DSS treatment [$F(101,0) = 4.4$; $p < 0.0001$], and for the DSS versus luteolin treatment interaction [$F(4,92) = 4.3$; $p = 0.0012$]). Furthermore, luteolin also completely prevented colonic hypersensitivity of DSS male mice 1 week post-DSS (Figures 5A and 5B, DSS treatment [$F(4,47) = 9.9$; $p < 0.0001$] and DSS versus luteolin treatment [$F(5,40) = 9.9$; $p < 0.0001$]) and eliminated depression-like behavior in the FST (Figure 5C, DSS treatment [$F(1,02) = 7.12$; $p = 0.0008$] and DSS versus luteolin treatment [$F(1,78) = 9.12$; $p = 0.0021$]) and TST (Figure 5D DSS treatment [$F(1,91) = 5.5$; $p = 0.0051$] and DSS versus luteolin treatment [$F(5,98) = 5.5$; $p = 0.0069$]), 4 weeks post-DSS. There was no effect on the number of crossings in the open field test (Figure S3), suggesting that locomotor dysfunctions are not major confounding factors in the interpretation of depression behaviors. We do acknowledge, however, that the FST and TST solicit abdominal muscles, which may be hypercontractile in visceral pain. Although the open-field test is not designed to detect such changes, we do note that there is likely no visceral hypersensitivity at the 4-week time point.

Luteolin Protects the Leaking Gut

Treatment of mice with DSS resulted in a decrease in transepithelial electrical resistance (TER), compared with controls 1 week from DSS discontinuation. TER is a widely used technique to quantify and determine the integrity of endothelial and epithelial tissues (Srinivasan et al., 2015). Luteolin treatment partially rescued the DSS-induced decrease in gut resistance of colitis mice with effect evident at 50 and 60 min. DSS-treated group exhibited decreased TER in colons mounted in Ussing chambers (Figure 6). Two-way RM ANOVA showed statistical difference in response to DSS treatment ($F(4,17) = 12.12$; $p < 0.0001$) and

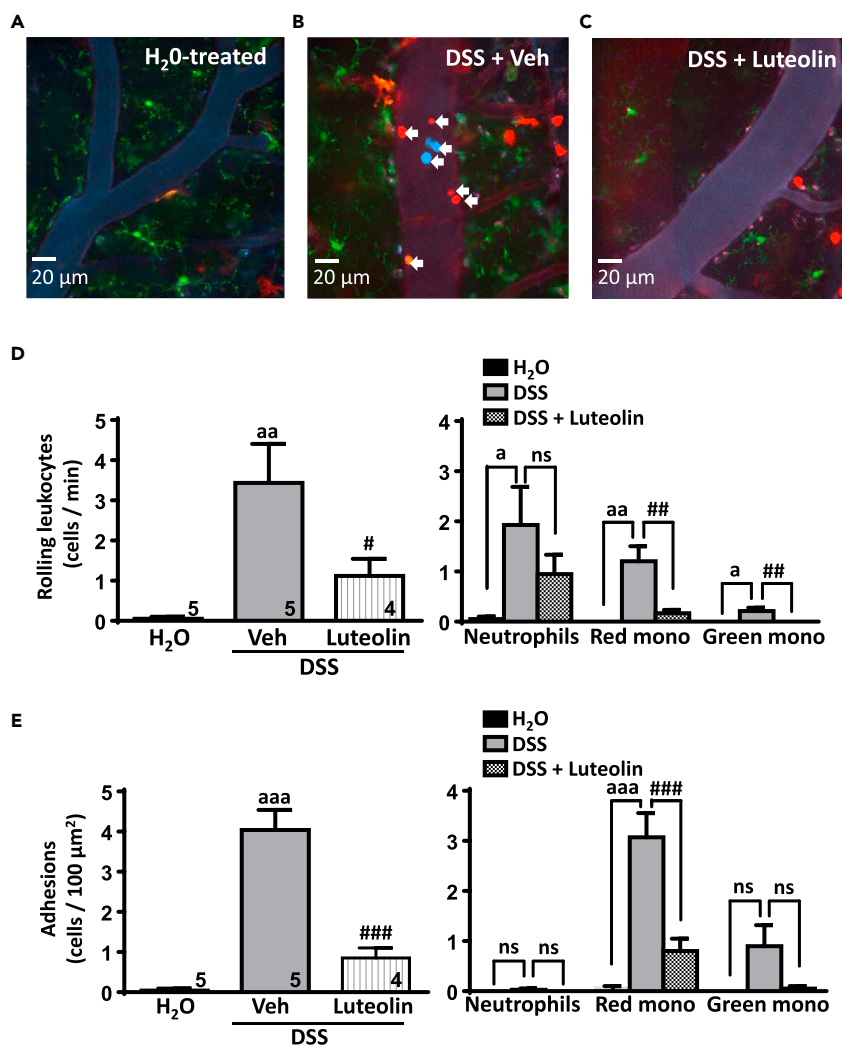


Figure 4. Imaging of Infiltrating Leukocytes into the Brain Microcirculation

(A–C) Intravital microscopy images of prefrontal cortex (PFC) vasculature performed 1 week after DSS discontinuation of (A) control (H₂O), (B) colitis (DSS + vehicle), and (C) colitis group treated with luteolin (15 mg/kg, intraperitoneally daily, 15 days starting 2 days before DSS treatment) in reporter mice CX3CR1^{GFP/WT}CCR2^{RFP/WT}. Neutrophils are labeled in blue, CCR2 inflammatory monocytes are labeled in red, and CX3CR1 patrolling monocytes are shown in green.

(D) Quantification of total (left) and differentiated (right) rolling leukocytes.

(E) Quantification of total (left) and differentiated (right) adherent leukocytes. Neutrophils are visualized in blue as detected by anti-Ly6G monoclonal antibody (mAb) (shown by arrows), CCR2⁺ monocytes are visualized red (shown by arrows), endothelium is visualized in red by anti-CD31 mAb, and microglia are visualized in green. Each bar represents the mean ± SEM (n = 4–5). Two-way ANOVA reveals an increased presence of leukocytes in the brain vasculature of DSS-treated mice and protective effect of luteolin treatment. ^ap < 0.05, ^{aa}p < 0.01, ^{aaa}p < 0.001 DSS- versus H₂O-treated mice; [#]p < 0.05, ^{##}p < 0.01, ^{###}p < 0.001 luteolin- versus vehicle-treated mice.

for the DSS versus luteolin treatment interaction ($F(1,74) = 12.12$; $p < 0.0001$). These data thus suggest that the increased gut permeability during colitis can be partially reversed with luteolin.

DISCUSSION

Inflammation and the immune system have emerged as important components of MDD (Hodes et al., 2015) and are thought to serve as an induction mechanism of depression-related behaviors (Walker et al., 2013). Our data reveal that behavioral abnormalities also arise following acute inflammation of the gut and are associated with changes in electrophysiological properties of the hippocampus and activation of

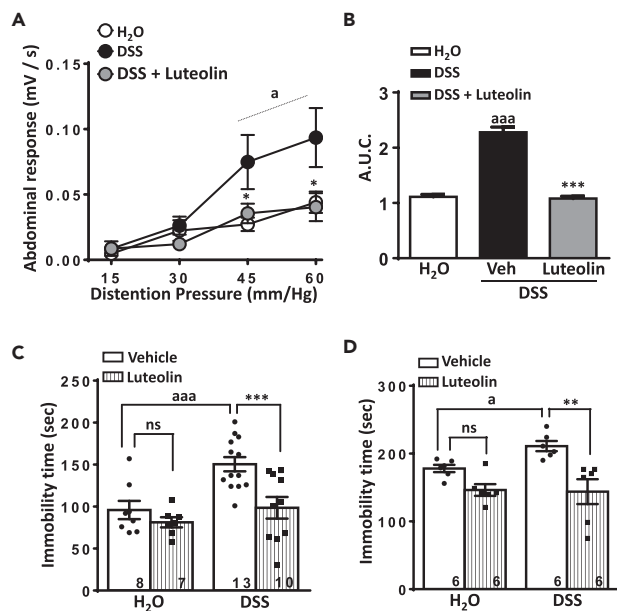


Figure 5. Luteolin Prevents Leukocyte Infiltration, Visceral Hypersensitivity, and Depression-like Behavior

Luteolin (15 mg/kg, intraperitoneally [i.p.] daily, 15 days) abolishes colonic hypersensitivity evaluated 6–7 days after DSS discontinuation in male mice.

(A–D) (A) Abdominal response and (B) area under the curve. Abdominal muscle contraction was recorded in response to distention pressures of 15, 30, 45, and 60 mm Hg. Each circle represents the mean \pm SEM. ($n = 10$ –11). Two-way RM ANOVA shows that luteolin completely abolishes colonic sensitivity of DSS-treated mice. ^a $p < 0.05$ DSS- versus H₂O-treated mice; ^{*} $p < 0.05$ luteolin- versus vehicle-treated mice. Antidepressant-like effect of luteolin (15 mg/kg, i.p. daily, 15 days) following inflammatory colitis in male mice in the (C) FST and (D) TST. Bars represent the mean \pm SEM and are representative of three experimental runs. Two-way ANOVA reveals antidepressant-like effect of luteolin. ^a $p < 0.05$, ^{aaa} $p < 0.001$ H₂O- versus DSS-vehicle mice; ^{**} $p < 0.01$, ^{***} $p < 0.001$ luteolin- versus vehicle-treated mice.

neuroimmune responses. The persistent upregulation of IL-1 β levels observed in our study is consistent with multiple reports implicating this cytokine in depression and suggests a sustained neuroinflammatory process following peripheral inflammation that can be mediated by circulating leukocytes.

Although microglia are well characterized as an important source of IL-1 β during neuroinflammation (Liu and Quan, 2018), our flow cytometry analysis suggests a different source other than the resident microglia in the brain for the elevated levels of IL-1 β in the hippocampus. Our *in vivo* intravital microscopic studies revealed an increase in the infiltration of neutrophils and monocytes of both subtypes into cerebral microvasculature, which are consistent with the higher levels of IL-1 β that we observed. After peripheral trauma or infection, neutrophils increase in number, and this is followed by an increase in monocytes that are recruited to the site of inflammation (Ginhoux and Jung, 2014). Neutrophil recruitment is initiated by changes in the surface of the endothelium as a result of stimulation by inflammatory mediators released from tissue-resident sentinel leukocytes. Neutrophils then facilitate the recruitment of monocytes into inflamed tissues (Kolaczowska and Kubes, 2013). Monocytes might further contribute to inflammation but may also partake in its resolution (Ginhoux and Jung, 2014). These cells are able to re-enter the vasculature where they may be involved in spreading the inflammatory processes to other organs (Kolaczowska and Kubes, 2013; de Oliveira et al., 2016), including immune-privileged sites, such as the brain (Shechter et al., 2013). The correlation between the peripheral immune system and depression is further supported by early studies showing increased neutrophils and Ly6C^{hi} monocytes in the blood of patients diagnosed with MDD (Smith, 1991; Maes, 1995) and by a more recent postmortem study that revealed an elevated number of peripheral monocytes in the brains of patients with depression (Torres-Platas et al., 2014).

The connection between depression and visceral inflammation appears to be bidirectional. In a mouse depression model based on reserpine-induced monoamine depletion, depression aggravated intestinal inflammation by altering tonic vagal inhibition of inflammatory cytokines (Ghia et al., 2008). Along these

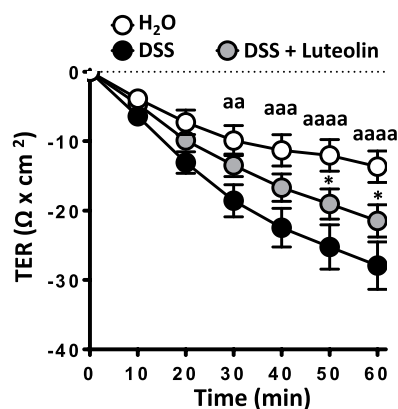


Figure 6. Luteolin Reverses DSS-Induced Changes in Gut Permeability

Luteolin attenuates intestinal epithelial barrier dysfunction induced by DSS in mice. The distal colon was mounted in Ussing chambers after luteolin treatment (15 mg/kg, intraperitoneally daily, 15 days), and TER was measured for 60 min 1 week after DSS discontinuation. Circles represent mean \pm SEM (n = 9–11). Two-way RM ANOVA reveals a significant effect of luteolin treatment. ^{aa}p < 0.01, ^{aaa}p < 0.001, ^{aaaa}p < 0.0001 H₂O- versus DSS- treated groups; *p < 0.05 luteolin- versus vehicle-treated groups.

lines, depression induced by either bulbectomy or reserpine reactivates inflammation following chronic colitis (Ghia et al., 2009). Stress was also found to induce immune reactions and alter gut microbiota, thus sensitizing DSS-treated mice and modulating mood behaviors, along with increased infiltration of B cells, neutrophils, and proinflammatory macrophages in colonic lamina propria (Gao et al., 2018). On the other hand, acute colitis in rats induced by DSS produced both pain and anxious depressive behaviors when assessed 1–2 weeks following DSS discontinuation (Chen et al., 2015), which is qualitatively consistent with our findings presented here.

It is estimated that 30%–50% of patients with depression are refractory to treatment with classical antidepressants, thus it becomes evident that distinct mechanisms are involved in this pathology (Krishnan and Nestler, 2008) and highlights the necessity of alternative strategies for therapeutic interventions. In this context, bioflavonoids have emerged as natural sources for new therapeutics (Katiyar et al., 2012). Luteolin is a flavone present in medicinal plants, vegetables, and fruits, such as peppermint, artichoke, celery, broccoli, onions, and peppers among others (Aziz et al., 2018). Besides its anti-oxidant, anti-microbial, anti-diabetic, anti-allergic, and neuroprotective actions, luteolin has potent anti-inflammatory properties *in vivo* and *in vitro* mainly due to inhibition of nitric oxide production and the expression of nuclear factor NF- κ B, which controls the production of inflammatory cytokines such as IL-1 β (Seelinger et al., 2008; Aziz et al., 2018). Luteolin has been reported to be neuroprotective and to have antidepressant-like action when delivered orally to mice (Ishisaka et al., 2011). It also produced analgesia in an animal model of neuropathic pain when delivery spinally, but not supraspinally (Hara et al., 2014). Luteolin treatment did not inhibit neutrophil migration to the colon of DSS mice when analyzed 1 week following DSS discontinuation (data not shown); however, the intestinal anti-inflammatory action of luteolin was previously described in DSS-treated mice. Following systemic delivery, luteolin inhibited macrophage infiltration into the colonic mucosa, produced anti-inflammatory activity in the intestine, and improved disease activity index (DAI), such as colon shortening and histological damage assessments (Nishitani et al., 2013). It also significantly reduced DAI in the colon of DSS-treated mice; reduced the expression of mRNA for several pro-inflammatory mediators such as iNOS, TNF- α , and IL-6; and increased the activities of colonic antioxidant factors such as Nrf2, SOD, and CAT (Li et al., 2016). These data are consistent with our findings showing that repeat dosing of systemically delivered luteolin prevents leukocyte infiltration into the brain, abolishes visceral hypersensitivity, and prevents the development of abnormal behaviors associated with depression.

Altogether, our findings reveal that acute visceral inflammation results in increased infiltration of leukocytes into the brain microvasculature and gives rise to depression-like behavior that is consistent with sustained neuroinflammation. Protecting the inflamed gut with the flavonoid luteolin prevents gut leakage and reverses behavioral abnormalities such as pain and depression. Thus the present study sheds light into the mechanisms that underlie the development of these comorbid conditions and suggest new ways for therapeutic intervention for the treatment of depression associated with visceral inflammation.

Limitations of the Study

It is important to recognize that the DSS model does not entirely reflect the etiology of human colitis (Chassaing et al., 2014). A second caveat is that although we examine changes in hippocampal function at the

cellular level, the intravital microscopic experiments do not allow access to deep brain structures such as the hippocampus, and instead are conducted in the PFC. We believe that the findings obtained in this brain structure are also relevant to hippocampal function.

METHODS

All methods can be found in the accompanying [Transparent Methods](#) supplemental file.

DATA AND SOFTWARE AVAILABILITY

RNA-seq Datasets Are Described in [Transparent Methods](#).

SUPPLEMENTAL INFORMATION

Supplemental Information can be found online at <https://doi.org/10.1016/j.isci.2019.05.012>.

ACKNOWLEDGMENTS

This work was supported by a foundation grant to G.W.Z. from the Canadian Institutes of Health Research (CIHR). S.M.D. is supported by an Alberta Innovates Fellowship. G.W.Z., C.A., and P.K. are Canada Research Chairs.

AUTHOR CONTRIBUTIONS

V.M.G. conceptualized the study, designed experiments, performed and analyzed experiments, and drafted the manuscript. G.A., Z.Z., S.M.D., C.H.B., and L.C. performed the experiments. L.B., C.A., P.K., and W.K.M.N. contributed technical expertise. G.W.Z. supervised the study and co-wrote the manuscript.

DECLARATION OF INTERESTS

The authors declare no competing interests.

Received: October 22, 2018

Revised: March 9, 2019

Accepted: May 9, 2019

Published: June 28, 2019

REFERENCES

- Alcocer-Gómez, E., Casas-Barquero, N., Williams, M.R., Romero-Guillena, S.L., Cañadas-Lozano, D., Bullón, P., Sánchez-Alcazar, J.A., Navarro-Pando, J.M., and Cordero, M.D. (2017). Antidepressants induce autophagy dependent-NLRP3-inflammasome inhibition in Major depressive disorder. *Pharmacol. Res.* **121**, 114–121.
- Andonegui, G., Zelinski, E.L., Schubert, C.L., Knight, D., Craig, L.A., Winston, B.W., Spanswick, S.C., Petri, B., Jenne, C.N., Sutherland, J.C., et al. (2018). Targeting inflammatory monocytes in sepsis-associated encephalopathy and long-term cognitive impairment. *JCI Insight* **3**, e99364.
- Aziz, N., Kim, M.Y., and Cho, J.Y. (2018). Anti-inflammatory effects of luteolin: a review of in vitro, in vivo, and in silico studies. *J. Ethnopharmacol.* **225**, 342–358.
- Bao, C.H., Liu, P., Liu, H.R., Wu, L.Y., Jin, X.M., Wang, S.Y., Shi, Y., Zhang, J.Y., Zeng, X.Q., Ma, L.L., et al. (2016). Differences in regional homogeneity between patients with Crohn's disease with and without abdominal pain revealed by resting-state functional magnetic resonance imaging. *Pain* **157**, 1037–1044.
- Batti, L., and O'Connor, J.J. (2010). Tumor necrosis factor- α impairs the recovery of synaptic transmission from hypoxia in rat hippocampal slices. *J. Neuroimmunol.* **218**, 21–27.
- Boddum, K., Jensen, T.P., Magloire, V., Kristiansen, U., Rusakov, D.A., Pavlov, I., and Walker, M.C. (2016). Astrocytic GABA transporter activity modulates excitatory neurotransmission. *Nat. Commun.* **25**, 13572.
- Chassaing, B., Aitken, J.D., Malleshappa, M., and Vijay-Kumar, M. (2014). Dextran sulfate sodium (DSS)-induced colitis in mice. *Curr. Protoc. Immunol.* **104**. Unit 15.25. <https://doi.org/10.1002/0471142735.im1525s104>.
- Chen, J., Winston, J.H., Fu, Y., Guptarak, J., Jensen, K.L., Shi, X.Z., Green, T.A., and Sarna, S.K. (2015). Genesis of anxiety, depression, and ongoing abdominal discomfort in ulcerative colitis-like colon inflammation. *Am. J. Physiol. Regul. Integr. Comp. Physiol.* **308**, 18–27.
- Costa, R., Motta, E.M., Manjavachi, M.N., Cola, M., and Calixto, J.B. (2012). Activation of the α -7 nicotinic acetylcholine receptor (α 7 nAChR) reverses referred mechanical hyperalgesia induced by colonic inflammation in mice. *Neuropharmacology* **63**, 798–805.
- Dantzer, R., O'Connor, J.C., Freund, G.G., Johnson, R.W., and Kelley, K.W. (2008). From inflammation to sickness and depression when the immune system subjugates the brain. *Nat. Rev. Neurosci.* **9**, 46–56.
- de Oliveira, S., Rosowski, E.E., and Huttenlocher, A. (2016). Neutrophil migration in infection and wound repair: going forward in reverse. *Nat. Rev. Immunol.* **16**, 378–391.
- Do, J., and Woo, J. (2018). From gut to brain: alteration in inflammation markers in the brain of dextran sodium sulfate-induced colitis model mice. *Clin. Psychopharmacol. Neurosci.* **16**, 422–433.
- Gao, X., Cao, Q., Cheng, Y., Zhao, D., Wang, Z., Yang, H., Wu, Q., You, L., Wang, Y., Lin, Y., et al. (2018). Chronic stress promotes colitis by disturbing the gut microbiota and triggering immune system response. *Proc. Natl. Acad. Sci. U S A* **115**, E2960–E2969.
- Ghia, J.E., Blennerhassett, P., and Collins, S.M. (2008). Impaired parasympathetic function

- increases susceptibility to inflammatory bowel disease in a mouse model of depression. *J. Clin. Invest.* 118, 2209–2218.
- Ghia, J.E., Blennerhassett, P., Deng, Y., Verdu, E.F., Khan, W.I., and Collins, S.M. (2009). Reactivation of inflammatory bowel disease in a mouse model of depression. *Gastroenterology* 136, 2280–2288.
- Ginhoux, F., and Jung, S. (2014). Monocytes and macrophages: developmental pathways and tissue homeostasis. *Nat. Rev. Immunol.* 14, 392–404.
- Hara, K., Haranishi, Y., Terada, T., Takahashi, Y., Nakamura, M., and Sata, T. (2014). Effects of intrathecal and intracerebroventricular administration of luteolin in a rat neuropathic pain model. *Pharmacol. Biochem. Behav.* 125, 78–84.
- Hodes, G.E., Kana, V., Menard, C., Merad, M., and Russo, S.J. (2015). Neuroimmune mechanisms of depression. *Nat. Neurosci.* 18, 1386–1393.
- Ikegaya, Y., Delcroix, I., Iwakura, Y., Matsuki, N., and Nishiyama, N. (2003). Interleukin-1 β abrogates long-term depression of hippocampal CA1 synaptic transmission. *Synapse* 47, 54–57.
- Ishisaka, M., Kakefuda, K., Yamauchi, M., Tsuruma, K., Shimazawa, M., Tsuruta, A., and Hara, H. (2011). Luteolin shows an antidepressant-like effect via suppressing endoplasmic reticulum stress. *Biol. Pharm. Bull.* 34, 1481–1486.
- Katiyar, C., Gupta, A., Kanjilal, S., and Katiyar, S. (2012). Drug discovery from plant sources: an integrated approach. *Ayu* 33, 10–19.
- Krishnan, V., and Nestler, E.J. (2008). The molecular neurobiology of depression. *Nature* 455, 894–902.
- Kolaczowska, E., and Kubes, P. (2013). Neutrophil recruitment and function in health and inflammation. *Nat. Rev. Immunol.* 13, 159–175.
- Li, Y., Shen, L., and Luo, H. (2016). Luteolin ameliorates dextran sulfate sodium-induced colitis in mice possibly through activation of the Nrf2 signaling pathway. *Int. Immunopharmacol.* 40, 24–31.
- Liu, X., and Quan, N. (2018). Microglia and CNS interleukin-1: beyond immunological concepts. *Front. Neurol.* 9, 8.
- Lopes, F., Keita, A.V., Saxena, A., Reyes, J.L., Mancini, N.L., Al Rajabi, A., Wang, A., Baggio, C.H., Dickey, M., van Dalen, R., et al. (2018). ER-stress mobilization of death-associated protein kinase-1-dependent xenophagy counteracts mitochondria stress-induced epithelial barrier dysfunction. *J. Biol. Chem.* 293, 3073–3087.
- López-Lázaro, M. (2009). Distribution and biological activities of the flavonoid luteolin. *Mini. Rev. Med. Chem.* 9, 31–59.
- Ma, X., Li, S., Tian, J., Jiang, G., Wen, H., Wang, T., Fang, J., Zhan, W., and Xu, Y. (2015). Altered brain spontaneous activity and connectivity network in irritable bowel syndrome patients: a resting-state fMRI study. *Clin. Neurophysiol.* 126, 1190–1197.
- Maes, M. (1995). Evidence for an immune response in major depression: a review and hypothesis. *Prog. Neuropsychopharmacol. Biol. Psychiatry* 19, 11–38.
- Murrough, J.W., Abdallah, C.G., and Mathew, S.J. (2017). Targeting glutamate signalling in depression: progress and prospects. *Nat. Rev. Drug Discov.* 16, 472–486.
- Nishitani, Y., Yamamoto, K., Yoshida, M., Azuma, T., Kanazawa, K., Hashimoto, T., and Mizuno, M. (2013). Intestinal anti-inflammatory activity of luteolin: role of the aglycone in NF- κ B inactivation in macrophages co-cultured with intestinal epithelial cells. *Biofactors* 39, 522–533.
- Seelinger, G., Merfort, I., and Schempp, C.M. (2008). Anti-oxidant, anti-inflammatory and anti-allergic activities of luteolin. *Planta Med.* 74, 1667–1677.
- Shechter, R., London, A., and Schwartz, M. (2013). Orchestrated leukocyte recruitment to immune-privileged sites: absolute barriers versus educational gates. *Nat. Rev. Immunol.* 13, 206–218.
- Smith, R.S. (1991). The macrophage theory of depression. *Med. Hypotheses* 35, 298–306.
- Spagnuolo, C., Moccia, S., and Russo, G.L. (2018). Anti-inflammatory effects of flavonoids in neurodegenerative disorders. *Eur. J. Med. Chem.* 153, 105–115.
- Srinivasan, B., Kolli, A.R., Esch, M.B., Abaci, H.E., Shuler, M.L., and Hickman, J.J. (2015). TEER measurement techniques for *in vitro* barrier model systems. *J. Lab. Autom.* 20, 107–126.
- Steru, L., Chermat, R., Thierry, B., and Simon, P. (1985). The tail suspension test: a new method for screening antidepressants in mice. *Psychopharmacology* 85, 367–370.
- Strober, W., and Fuss, I.J. (2011). Pro-inflammatory cytokines in the pathogenesis of IBD. *Gastroenterology* 140, 1756–1767.
- Torres-Platas, S.G., Cruceanu, C., Chen, G.G., Turecki, G., and Mechawar, N. (2014). Evidence for increased microglial priming and macrophage recruitment in the dorsal anterior cingulate white matter of depressed suicides. *Brain Behav. Immun.* 42, 50–59.
- Walker, A.K., Kavelaars, A., Heijnen, C.J., and Dantzer, R. (2013). Neuroinflammation and comorbidity of pain and depression. *Pharmacol. Rev.* 66, 80–101.
- Zonis, S., Pechnick, R.N., Ljubimov, V.A., Mahgerefteh, M., Wawrowsky, K., Michelsen, K.S., and Chesnokova, V. (2015). Chronic intestinal inflammation alters hippocampal neurogenesis. *J. Neuroinflammation* 12, 65.

ISCI, Volume 16

Supplemental Information

Neuroimmune Responses Mediate Depression-Related

Behaviors following Acute Colitis

Vinicius M. Gadotti, Graciela Andonegui, Zizhen Zhang, Said M'Dahoma, Cristiane H. Baggio, Lina Chen, Lilian Basso, Christophe Altier, Wallace K. MacNaughton, Paul Kubes, and Gerald W. Zamponi

Supplementary data:

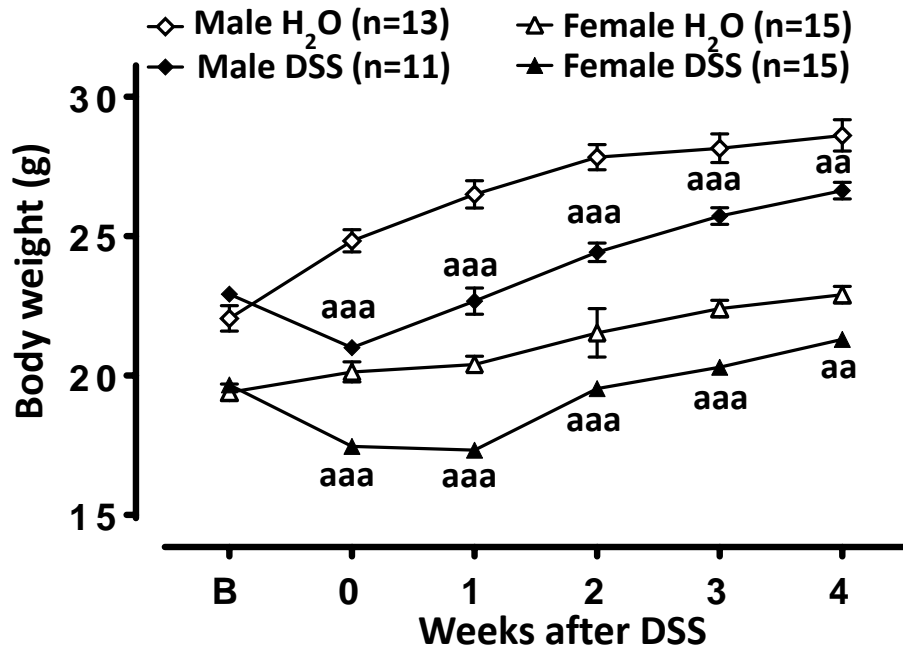
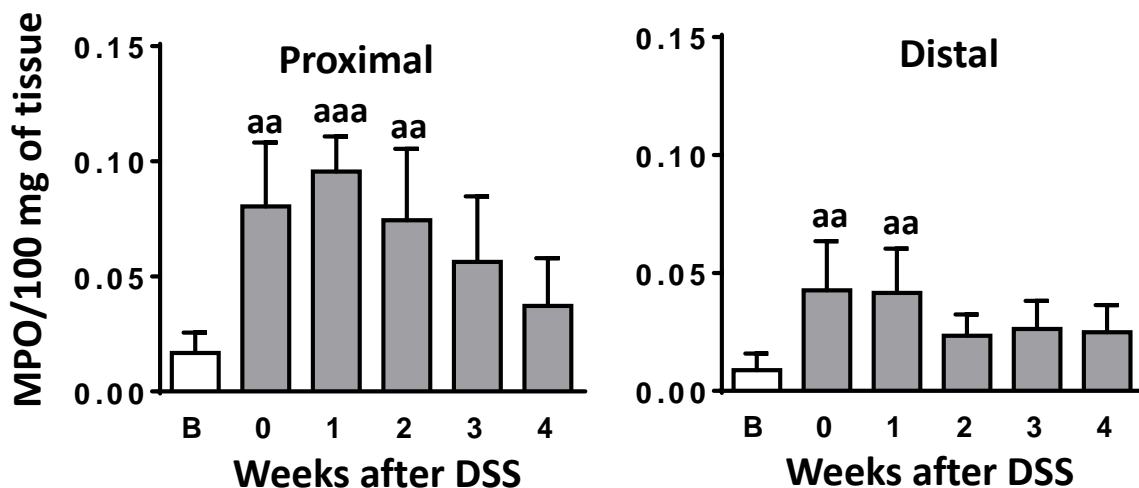
S1A**S1B**

Figure S1 (related to Fig. 1) (A) Time course of body weight loss of either male or female mice treated with DSS (2.5%) or water. Each circle represents the mean \pm SEM ($n = 11-15$) and is representative of two independent experiments. Three-way RM ANOVA revealed that the body weight of mice receiving DSS were significantly lower than those treated with water. (B) Time course of MPO activity in the proximal (right) and distal (left) colon of DSS treated mice. Bars represent the mean \pm S.E.M. ($n=5$) and are representative of 2 independent experiments.

S2

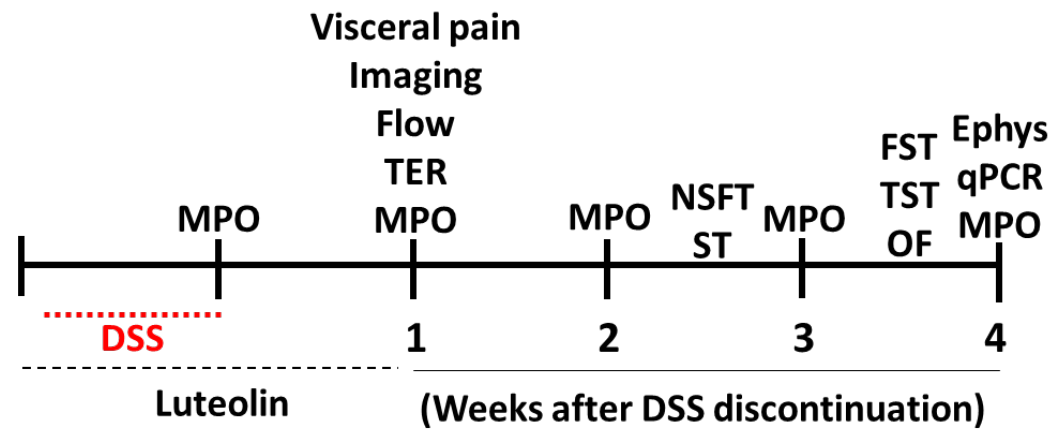


Figure S2 (related to all figures). Summary of time lines for the experiments conducted in this study. Abbreviations: DSS – dextran sulfate sodium; MPO – myeloperoxidase; TER – transepithelial resistance; NSFT – novelty suppressed feeding test; FST – forced swimming test; TST – tail suspension test; OF- open field, qPCR – quantitative polymerase chain reaction; Ephys – electrophysiology)

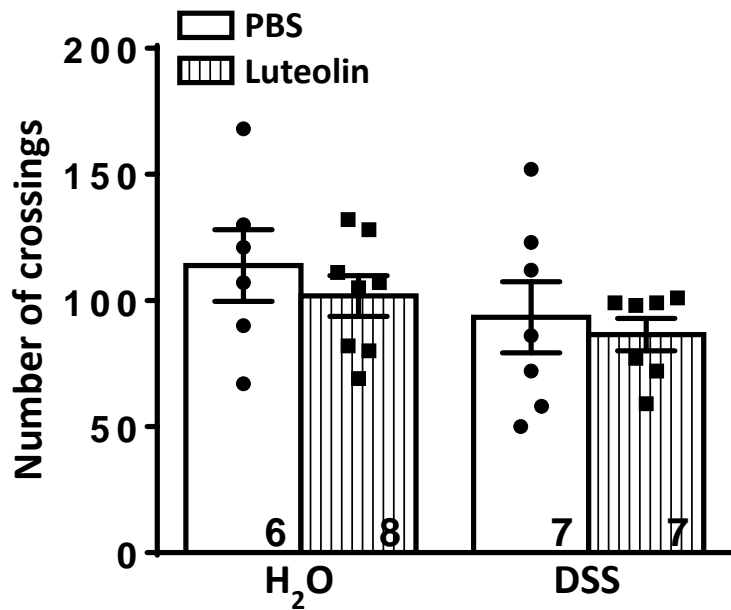
S3

Figure S3 (related to Fig. 4) Blinded assessment of ambulatory behaviour of male mice on the open field apparatus following inflammatory colitis and treatment with Luteolin (15 mg/kg, i.p. daily, 15 days). Bars represent the mean ± S.E.M. and are representative of 3 independent experiments (n=6-8 mice). Two-way ANOVA reveals no difference of crossing among groups.

Supplementary Video1 (related to Fig. 4):

Intravital microscopy of blood vessels in the prefrontal cortex of control mice. Neutrophils are labeled in blue, CCR2 inflammatory monocytes are labeled in red, CX3CR1 patrolling monocytes are shown in green.

Supplementary Video2 (related to Fig. 4):

Intravital microscopy of blood vessels in the prefrontal cortex of mice subjected to DSS treatment. Neutrophils are labeled in blue, CCR2 inflammatory monocytes are labeled in red, CX3CR1 patrolling monocytes are shown in green.

Supplementary Video3 (related to Fig. 4):

Intravital microscopy of blood vessels in the prefrontal cortex of DSS mice treated with Luteolin. Neutrophils are labeled in blue, CCR2 inflammatory monocytes are labeled in red, CX3CR1 patrolling monocytes are shown in green.

Transparent methods:**Animals**

Male or female adult mice (C57BL/6J) aged between 6-11 weeks were used and purchased from Jackson Laboratories. CX3CR1-GFP/CCR2-RFP (CX3CR1^{GFP/WT}CCR2^{RFP/WT}) reporter mice breeders were bred in-house.

Experiments were approved by the institutional animal care committee. Mice were kept in housing cages at a number of five per cage (30 x 20 x 15 cm) on a 12-hr light/dark cycle (lights on at 7am) at a temperature of 23 ± 1°C and with free access to water and food unless specified elsewhere. Experiments were carried out between 10am and 2pm. When the same cohorts of mice were used for behavioural analysis, they were tested first on the less stressful test and always obeying a 3 days minimum interval between testing sessions and each animal was tested only once (for example: they were first tested on the open field apparatus, then 3 days later tested on forced swimming test; or they were first tested on splash test, then tested on tail suspension test). Female and male mice were tested in separate groups. For cell biology experiments and behavioural assessments examining the *in vivo* actions of Luteolin or the positive control imipramine, only male mice were used. For all behavioural studies animals were tested in randomized trials.

Reagents and treatment

Dextran sodium sulfate (DSS, Affymetrix) was prepared in autoclaved water and administered in drinking water for 6 consecutive days. Luteolin (15 mg/kg, Tocris) and Imipramine (Sigma-Aldrich) were suspended in DMSO (5%), diluted in sterile PBS and administered intraperitoneally (i.p.). Luteolin was delivered chronically once

a day for 15 days starting 2 days before beginning of the 6 days DSS treatment protocol.

Colorectal distention and electromyographic recording

Evaluation of colonic hypersensitivity was performed as pain index. Three days prior to colorectal distention, two electrodes were implanted in the abdominal external oblique musculature of mice anesthetized Isoflurane. Electrodes were exteriorized at the back of the neck and protected by a plastic tube attached to the skin. In the experimental day, animals were allowed to acclimate in the room and implanted electrodes were connected to a Bio Amp, which was connected to an electromyogram acquisition system (AD Instruments, Inc, Colorado Springs, CO). A Fogarty thru-lumen embolectomy catheter 4F (Edward Lifesciences) was gently inserted into the colon at 5 mm proximal to the rectum. The balloon was inflated in a stepwise fashion. Ten second distentions were performed at pressures of 15, 30, 45, and 60 mm/Hg with 5-10 minute rest intervals. Electromyographic activity of the abdominal muscles was recorded and visceromotor responses were calculated using LabChart 8 software (ADInstruments).

Novelty suppressed feeding test

This test is used specifically for evaluating levels of anhedonia as a feature of depression. Animals were food-deprived for 24 h and thereafter introduced to a novel 40 x 60 x 50 cm arena with wood shavings floor (same as housing cages) and with a single pellet of food placed in the centre of the arena. Animals were individually placed in a corner of the arena backwards to the walls and the latency of each

mouse to interact with the food pellet was recorded. After the test, animals were immediately returned to its home cage.

Splash test

The Splash Test is based on grooming behaviour and used to access depressive-like behaviour of mice. The grooming behaviour was scored during 5 min after spraying a 10% sucrose solution on the dorsal coat of the mice.

Forced swimming test

Mice were individually allowed to swim in an open cylindrical container (diameter 10cm x height 25cm), containing 19 cm of water at 24 ± 1 °C; the total duration of immobility during a 6 min test was scored. A mouse was considered to be immobile when it stops moving its limbs in any kind of swimming action and remains motionless floating in the water, while making the necessary movements with its tail to keep the head above the water. Immobility time was timed for the entire 6 min they spend in the water. Animals were never allowed to drown during the test.

Tail suspension test

Mice were both acoustically and visually isolated and individually suspended 50cm above the floor with adhesive tape placed approximately 1cm from the tip of the tail. Immobility time of mice was quantified when a mouse stopped struggling and remained without any body movement (total immobility time) for 6 min.

Open field test

An open field test was used exclusively to assess locomotor activity of mice to validate the forced swimming and tail suspension tests. The apparatus consists of a wooden box measuring 40 × 60 × 50 cm with a frontal glass wall. The floor of the arena is divided into 12 equal squares and placed in a sound free room. Animals were placed in the rear left square and allowed to explore freely for 6 minutes. Crossings reflect the number of grid lines that were crossed with all paws (crossing). The apparatus was cleaned with a 70% alcohol solution and dried after each individual mouse session.

Electrophysiological recording (eIPSCs) of CA1 pyramidal cells

Four weeks after discontinuation of DSS treatment, acute coronal brain slices (300 μm) containing CA1 region were obtained from C57BL/6J (DSS- or H₂O- treated) mice using a vibratome (Leica VT1200S, Leica Biosystems) in an ice-cold NMDG-based solution (Ting et al., 2014). Brain slices were first incubated at 33.5°C in NMDG-based solution for 11 min, then in normal external solution for 50 min, and finally transferred to room temperature in normal external solution for at least 1hr before recording. Whole cell patch clamp recordings were performed in pyramidal neurons (pyramidal layer) in CA1 area using MultiClamp 700B and Digidata 1440A (Molecular Devices). Normal external solution contained (mM): NaCl 120, NaH₂PO₄ 1.25, NaHCO₃ 26, Glucose 25, CaCl₂ 2.5, KCl 2.5, MgSO₄·7H₂O 1.3. The intracellular solution for voltage clamp was Cs-Methanesulfonate based (mM): Cs-Meth 130, CsCl 4, EGTA 2, ATP-Mg 4, GTP-Na 0.3, HEPES 10, QX314 5. Schaffer collaterals were stimulated using a bipolar concentric electrode placed in the stratum radiatum (100 μs pulses, 1-10 V, with 1 V increment) at 100-300 μm from the

recorded cells. Feedforward disynaptic inhibitory postsynaptic currents (IPSCs) were recorded at a holding potential of 0 mV (reversal potential of EPSC) in the absence of synaptic blockers. Brain slices were perfused with external solution at 32-33°C. All chemicals were purchased from Sigma.

Real time quantitative RT-PCR measurements

Mice were killed by decapitation and hippocampi were rapidly dissected at 0-4 °C and immediately flash frozen to be stored at -80 °C. Total RNA was extracted using the NucleoSpin RNA II extraction kit (Macherey-Nagel) and quantified using a NanoDrop. First-stranded cDNA synthesis (from 1 µg total RNA per 20 µl of reaction mixture) was carried out using QuantiTect® Reverse Transcription Kit (Qiagen). PCR amplification, in triplicate for each sample, was performed using the QuantStudio 3 Real-Time PCR System and TaqMan® Universal PCR Master Mix No AmpErase® UNG (Thermo Fisher Scientific). Semi-quantitative determinations were made for the target genes IL1-beta (Mm00434228_m1) and TNF-alpha (Mm00443258_m1) with reference to the reporter genes encoding GAPDH (Mm99999915_g1) and ACTB (Mm00607939_s1). The polymerase activation step at 95°C for 15 min was followed by 40 cycles of 15 s at 95°C and 60 s at 60°C. The validity of the results was checked by running appropriate negative controls (replacement of cDNA by water for PCR amplification; omission of reverse transcriptase for cDNA synthesis). Specific mRNA levels were calculated after normalizing from GAPDH and ACTB mRNA in each sample using the 2^{(-Delta C(T))} method. Data are presented as relative mRNA units compared to control values.

Flow cytometry

Assessment of microglia activation by flow-cytometry was performed in brain cells isolated using a previously described protocol (Andonegui et al., 2018). The samples were analyzed on a BD FACSCanto™ flow-cytometer using FACSDiva™ Software and FlowJo Software (BD Biosciences, Franklin Lakes, NJ, USA). The expression of CD11b coupled with the differential expression of CD45 antigen was used to distinguish between resting/activated microglia and cerebral infiltrating monocytes. Resting and activated microglia were defined as CD45^{low} CD11b⁺ and CD45^{intermediate} CD11b⁺ cells, respectively; monocytes are defined as CD45^{high} CD11b⁺ cells.

Intravital imaging

Intra-vital microscopy was performed using established procedures and according to Andonegui and colleagues (Andonegui et al., 2018). Mice were anesthetized via intraperitoneal delivery of 200 mg/kg ketamine and 10 mg/kg of xylazine. The jugular vein was then cannulated to administer labeled antibodies. Mice were positioned under an infrared heat lamp to maintain body temperature and their heads were shaved prior to craniotomy using a high-speed drill. After removal of the dura mater the brain was alive and fully perfused, and the animals were placed on an upright spinning disk confocal microscope. Neutrophils in the brain microvasculature were visualized using an anti-mouse Ly6G mAb conjugated to APC (clone 1A8, BioLegend, San Diego, CA, USA). The vascular endothelium was visualized using anti-mouse CD31 mAb conjugated to PE (clone 390, eBiosciences, San Diego, CA, USA). The antibodies were delivered via intravenous injection. CCR2 positive inflammatory monocytes and CX3CR1 positive patrolling monocytes were identified

in heterozygous CX3CR1^{GFP/WT}CCR2^{RFP/WT} knock-in mice using an Olympus BX51WI upright microscope. The instrument is equipped with a confocal light path based on a modified Yokogawa CSU-X1 head with a 20x/0.95W(LUMPLANFL) water immersion objective. Up to three laser excitation wavelengths (491, 561, and 640 nm; Cobalt) were used in rapid succession for imaging of the three types of immune cells. A back-thinned EM-CCD 512 × 512 pixel camera was used for fluorescence detection. Volocity® software was used for acquisition and analysis. The number of rolling and adherent neutrophils and monocytes were determined offline. Adherent neutrophils and monocytes were considered the cells that remained stationary for longer than 30 seconds.

Ussing chambers and transepithelial electrical resistance (TER)

Mice were euthanized, distal colons were removed, and opened longitudinally along the mesenteric border. They were rinsed in cold (4°C) Krebs buffer (pH 7.4) and mounted in Ussing chambers (Physiologic Instruments, San Diego, CA). The apical side was bathed with Krebs buffer containing 10 mM mannitol, while the serosal side was bathed with Krebs buffer containing 10 mM glucose. Tissues were maintained at 37°C and bubbled with 95% O₂-5% CO₂. Short-circuit current (I_{sc}) was measured under voltage clamp (0 V) conditions, with 5 mV pulses applied every 20 s so that TER could be measured concurrently (Acquire and Analyze software, Physiologic Instruments).

Determination of myeloperoxidase (MPO) activity

MPO activity (a marker of neutrophil infiltration) was measured according to a protocol previously described (De Young et al., 1989). Colons were homogenized

with 220 mM sodium phosphate, pH 7.4 and centrifuged at $9,000 \times g$ for 20 min at 4 °C. The pellet was re-suspended in 80 mM sodium phosphate buffer (pH 5.4) containing 0.5% hexadecyltrimethylammonium bromide (HTAB), and again centrifuged at $11,000 \times g$ for 20 min at 4 °C. MPO activity of supernatants was determined at 650 nm in presence of 0.017% H₂O₂ and 3,3',5,5'-tetramethylbenzidine (TMB, 18.4 mM) and expressed as MPO activity/100 mg of tissue.

Statistical analysis

Data were analyzed with Graphpad Prism 6.0., Synaptosoft or Clampfit and are presented as the mean \pm SEM. *In vivo* and intravital microscopy data were analyzed by one- or two-way analysis of variance (ANOVA) or by Repeated Measures (RM) ANOVA followed by a Newman-Keuls post hoc test. Unpaired *t* tests and one way ANOVA with Bonferroni's correction for multiple comparisons tests were used in comparison of electrophysiological data. Evoked IPSC (eIPSC) data were analyzed using the Mini Analysis Program (Synaptosoft) and Clampfit (Molecular Devices). Unpaired *t* tests were also used for analysis of qPCR data. For gut permeability and MPO assays statistical analysis were performed using two-way ANOVA followed by Dunnett's multiple comparison test. Statistical significance was accepted at the level of $p < 0.05$.

Supplemental References

Andonegui, G., Zelinski, E.L., Schubert, C.L., Knight, D., Craig, L.A., Winston, B.W., Spanswick, S.C., Petri, B., Jenne, C.N., Sutherland, J.C., et al., (2018). Targeting inflammatory monocytes in sepsis-associated encephalopathy and long-term cognitive impairment. *JCI Insight* 3, e99364.

De Young, L.M., Kheifets, J.B., Ballaron, S.J., and Young, J.M. (1989). Edema and cell infiltration in the phorbol ester-treated mouse ear are temporally separate and can be differentially modulated by pharmacologic agents. *Agents Actions* 26, 335-341.

Ting, J.T., Daigle, T.L., Chen, Q., and Feng, G. (2014). Acute brain slice method for adult and aging animals: application of targeted patch clamp analysis and optogenetics. *Methods Mol. Biol.* 1183, 221–242.